Crossovers and critical scaling in the one-dimensional transverse-field Ising model

Jianda Wu, Lijun Zhu, and Qimiao Si

Phys. Rev. B **97**, 245127 — Published 18 June 2018

DOI: 10.1103/PhysRevB.97.245127

Crossovers and critical scaling in the one-dimensional transverse field Ising model

Jianda Wu,[1,2] Lijun Zhu,[3] and Qimiao Si[4]

[1]*Department of Physics & Astronomy, Rice University, Houston, Texas 77005, USA*
[2]*Max-Planck-Institut für Physik komplexer Systeme, Dresden, 01187, Germany*
[3]*Department of Physics and Astronomy, University of California, Riverside, CA 92521, USA*
[4]*Department of Physics & Astronomy and Rice Center for Quantum Materials, Rice University, Houston, Texas 77005, USA*

(Dated: June 5, 2018)

We consider the scaling behavior of thermodynamic quantities in the one-dimensional transverse field Ising model near its quantum critical point (QCP). Our study has been motivated by the question about the thermodynamical signatures of this paradigmatic quantum critical system and, more generally, by the issue of how quantum criticality accumulates entropy. We find that the crossovers in the phase diagram of temperature and (the non-thermal control parameter) transverse field obey a general scaling ansatz, and so does the critical scaling behavior of the specific heat and magnetic expansion coefficient. Furthermore, the Grüneisen ratio diverges in a power-law way when the QCP is accessed as a function of the transverse field at zero temperature, which follows the prediction of quantum critical scaling. However, at the critical field, upon decreasing the temperature, the Grüneisen ratio approaches a constant instead of showing the expected divergence. We are able to understand this unusual result in terms of a peculiar form of the quantum critical scaling function for the free energy; the contribution to the Grüneisen ratio vanishes at the linear order in a suitable Taylor expansion of the scaling function. In spite of this special form of the scaling function, we show that the entropy is still maximized near the QCP, as expected from the general scaling argument. Our results establish the telltale thermodynamic signature of a transverse-field Ising chain, and will thus facilitate the experimental identification of this model quantum-critical system in real materials.

I. INTRODUCTION

Quantum phase transition arises in a many-body system at zero temperature, when the energy of its ground state is tuned by a non-thermal parameter to a point of non-analyticity[1–4]. When a transition is continuous, it describes a quantum critical point (QCP). The interplay between thermal and quantum fluctuations strongly influences physical properties near a QCP.[5–11]. In this context, an important thermodynamic quantity is the Grüneisen ratio[12] — the ratio of the thermal expansion coefficient to the specific heat. Ref. [13] advanced a quantum critical scaling form for the free energy, and demonstrated that the Grüneisen ratio diverges. This divergence is to be contrasted with the case of the classical (*i.e.* thermally-driven) critical point, where the Grüneisen ratio remains finite[12,14]. The divergence of the Grüneisen ratio has been experimentally observed in heavy fermion metals[15]. Indeed, such a divergence has been established as a means of diagnosing quantum criticality. An important consequence of this divergence is that the entropy is maximized near the QCP[13,16], which has recently been directly shown experimentally in several quantum critical materials, including $Sr_3Ru_2O_7$[17] and $CeCu_{6-x}Au_x$[18].

In this paper we focus on the one-dimensional transverse field Ising model (1DTFIM) – a paradigmatic system for quantum criticality[19–26]. The 1DTFIM and its related one-dimensional models remain a topic of considerable interest[27–35]. The 1DTFIM undergoes a continuous quantum phase transition when the transverse field – defined as g – is tuned across its critical value, g_c. Near g_c, the correlation length diverges as $|g-g_c|^{-1}$, and the excitation gap closes as $|g-g_c|$ with the correlation length and dynamic critical exponents $\nu = z = 1$. The divergence of the correlation length implies the existence of long-range entanglement of the ground state wavefunction near the QCP, which is a linear-superposition of enormous possible product states of spins in the huge 2^N Hilbert space with N being the total number of sites of this thermodynamic system. This long range entanglement strongly influences the physics around the QCP, leading to a rich $T-g$ phase diagram shown in Fig. 1, where the crossover boundaries between the different

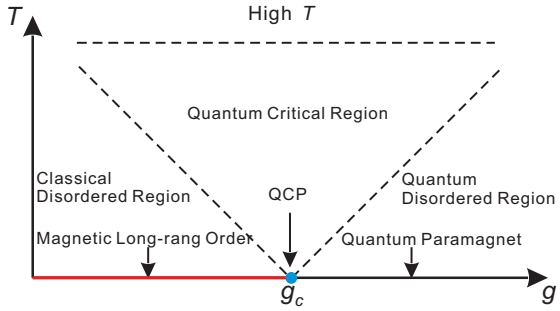

FIG. 1: The phase diagram of the 1DTFIM. g denotes the transverse field, with g_c being the QCP. The red solid line shows the ordered region at zero temperature. The two tilted dash lines illustrate crossover boundaries between different disordered regions at nonzero temperatures. The dashed line on the top silhouettes the crossover to the classical region at high temperatures.

regimes are characterized by $T \propto |g - g_c|$ [24].

The hyperscaling ansatz[13] leads to general statements about the crossover and scaling behavior of the thermodynamic quantities near a QCP. While such an analysis is very powerful, what the ansatz does not specify is the actual form of the scaling functions. In order to identify signatures that are unique to the 1DTFIM, here we systematically analyze such crossover and scaling properties by determining the scaling functions. We demonstrate that the entropy is indeed maximized near the QCP of the 1DTFIM. We also show that the specific heat and magnetic expansion coefficient [*c.f.* Eq. (1)] exhibit crossovers and scaling behavior compatible with the hyperscaling ansatz, but with some unique features that serve as telltale signs for the 1DTFIM. These features can be used to experimentally ascertain whether the 1DTFIM is realized in candidate materials.

The specific features we have identified are as follows. While the free energy for the 1DTFIM does obey the hyperscaling ansatz, there is an unusual contrast between the T and g dependencies of the Grüneisen ratio. We find that the Grüneisen ratio is power-law divergent when the system is tuned through the QCP at zero temperature by varying the transverse field, but approaches a finite constant when the QCP is reached with decreasing temperatures. The former respects the conventional analysis based on the hyperscaling ansatz[13,36]. The later, however, fails to display the expected singular behavior. We identify the origin of this special feature in the quantum critical region : In the 1DTFIM, the non-vanishing scaling term in this part of the phase diagram (*c.f.*, Fig. 1) begins at the second order.

The remainder of the paper is organized as follows. Sec. II is devoted to a general discussion of the critical scaling behaviors of the Grüneisen ratio near generic QCPs. Sec. III specifies the exact integral expressions for the thermodynamic quantities of the 1DTFIM. In Sec. IV, we determine the scaling function for the free energy of the 1DTFIM in the classical disordered, quantum disordered and quantum critical regions; in turn, we extract the analytic expressions that describe the critical scaling of various thermodynamic quantities. Sec. V presents the numerical results on the crossover scaling behaviors for these thermodynamic quantities, Sec. VI contains the discussions and conclusions.

II. THE GRÜNEISEN RATIO NEAR GENERIC MAGNETIC-FIELD-TUNED QCPS

When the control parameter is an external magnetic field H, the Grüneisen ratio is defined as[12–14]

$$\Gamma_H = \frac{\alpha_H}{c_H} = -\frac{1}{T}\frac{(\partial M/\partial T)_H}{(\partial S/\partial T)_H} = -\frac{1}{T}\frac{(\partial S/\partial H)_T}{(\partial S/\partial T)_H}, \quad (1)$$

where c_H, α_H, and S are the molar specific heat, magnetic expansion coefficient, and entropy, respectively. In addition M is the magnetization per mole. The scaling analysis leads to the expectation that the Grüneisen ratio is generically divergent at QCPs[13]. Since the effective dimension $(d + z)$ for the 1DTFIM is 2 $(d = 1, z = 1)$, the quantum criticality is expected to be non-Gaussian, and the hyperscaling hypothesis should work well for the model in the thermodynamic limit. In the hyperscaling ansatz, the critical behavior is governed by the correlation length along the space and time dimensions, ξ and ξ_τ, and the critical component of the free energy of a thermodynamic system near its critical point, F_{cr}, can be generally written as[13]

$$\frac{F_{cr}}{N} = -\rho_0 |r|^{\nu(d+z)} \tilde{f}\left(\frac{T}{T_0|r|^{\nu z}}\right) \quad (2)$$

$$= -\rho_0 \left(\frac{T}{T_0}\right)^{(d+z)/z} f\left(\frac{r}{(T/T_0)^{1/(\nu z)}}\right), \quad (3)$$

where ρ_0 and T_0 are nonuniversal constants; $r = (H - H_c)/H_c$ is the magnetic-field-tuning parameter normalized by the critical field H_c, shifted such that the QCP corresponds to $r = 0$ at $T = 0$; and $f(x)$ and $\tilde{f}(x)$ are universal scaling functions. It then follows that the Grüneisen ratio near a generic QCP has the following forms[13]

$$\Gamma_{cr}(T, r = 0) = \frac{\alpha_{cr}}{c_{cr}} = -G_T T^{-1/(\nu z)}, \quad (4)$$

$$\Gamma_{cr}(T \to 0, r) = -G_r \frac{1}{V_m(H - H_c)}, \quad (5)$$

where $G_T = \{[(d + z - 1/\nu)z f'(0)]/[d(d + z)f(0)]\}[T_0^{1/(\nu z)}/(H_c V_m)]$ and $G_r = \nu(d - y_0 z)/y_0$ with y_0 coming from the expansion of $\tilde{f}(x \to 0) = \tilde{f}(0) + cx^{y_0+1}$; y_0 is introduced to guarantee that the entropy vanishes in the zero temperature limit. It is expected that $G_r \leq 0$ due to the stronger competition in the quantum critical region between non-commutative fields than that in the disordered region[36]; this is indeed true for the 1DTFIM. Then from Eq. (5) one can observe that when the magnetic field H varies from values smaller to larger than H_c, the sign of the Grüneisen ratio changes from negative to positive. As a result, from the original definition of the Grüneisen ratio (Eq. (1)) the entropy at a low but nonzero temperature generally is maximized near the QCP. We shall explicitly demonstrate that Eq. (5) is correct for the 1DTFIM. By contrast, we will show that Eq.(4) does not hold in the 1DTFIM although the free energy follows the form of the hyperscaling ansatz.

III. THERMODYNAMIC QUANTITIES IN THE 1DTFIM

The 1DTFIM with nearest neighboring interaction corresponds to the following Hamiltonian,

$$H_I = -J \sum_i \left(g\hat{\sigma}_i^x + \hat{\sigma}_i^z \hat{\sigma}_{i+1}^z\right), \quad (6)$$

where the spins $S_i^\alpha = \frac{1}{2}\sigma_i^\alpha (\alpha = x, y, z)$ with σ_i^α and i denoting the Pauli matrices and the site positions, respectively. The nearest neighbor distance is set to 1. We consider ferromagnetic exchange interactions, with the nearest neighbor coupling J, between the Ising (z-) component of the spins, taken to be positive $J > 0$. In addition, gJ describes an external magnetic field for the transverse (x-) component of the spins. As is standard, after applying the Jordan-Wigner transformation,

$$\begin{cases} \sigma_i^x = 1 - 2c_i^\dagger c_i \\ \sigma_i^z = -\prod_{j<i}\left(1 - 2c_j^\dagger c_j\right)\left(c_i + c_i^\dagger\right) \end{cases}, \tag{7}$$

and Bogoliubov quasi-particle transformation $\gamma_k = u_k c_k - i v_k c_k^\dagger$ with conditions of $u_k^2 + v_k^2 = 1, u_{-k} = u_k$, $v_{-k} = -v_k$, and $c_k = \frac{1}{\sqrt{N}}\sum_j c_j e^{-ikj}$, one obtains a diagonalized Hamiltonian in the Bogoliubov quasi-particle representation,

$$H_I = \sum_k \varepsilon_k \left(\gamma_k^\dagger \gamma_k - 1/2\right) \tag{8}$$

with the single-particle spectrum $\varepsilon_k = 2J(1 + g^2 - 2g\cos k)^{1/2}$. It follows that the free energy density for the 1DTFIM, normalized by J, has the form[21,37]

$$f_I = \frac{F_I}{NJ} = -\frac{1}{\beta}\left[\ln 2 + \frac{1}{\pi}\int_0^\pi dk \ln\cosh\left(\frac{\beta\varepsilon_k}{2}\right)\right], \tag{9}$$

where the dimensionless temperature $t = k_B T/J$ and $\beta = 1/t$ are introduced for convenience. And the ε_k here and in the following does not contain the factor of J any more. With the free energy density Eq. (9), the (dimensionless) entropy $s = -(\partial f_I/\partial t)$, magnetic expansion coefficient $\alpha = -(\partial s/\partial g)_t$, and specific heat $c_v = t(\partial s/\partial t)_g$ are determined as follows

$$s = \ln 2 + \frac{1}{\pi}\int_0^\pi dk \left[\ln\cosh\left(\frac{\beta\varepsilon_k}{2}\right) - \frac{\beta\varepsilon_k}{2}\tanh\left(\frac{\beta\varepsilon_k}{2}\right)\right]; \tag{10}$$

$$\alpha = \frac{1}{\pi}\int_0^\pi dk \frac{g - \cos k}{t^2}\mathrm{sech}^2\left(\beta\varepsilon_k/2\right); \tag{11}$$

$$c_v = \frac{1}{\pi}\int_0^\pi dk (\beta\varepsilon_k/2)^2 \mathrm{sech}^2\left(\beta\varepsilon_k/2\right). \tag{12}$$

Armed with these expressions, we now turn to analyzing and discussing the crossover and critical scaling behaviors.

IV. SCALING BEHAVIORS OF THERMODYNAMIC QUANTITIES IN THE 1DTFIM

In this section, we discuss the scaling behaviors of thermodynamic quantities of the 1DTFIM in the classical disordered region (CDR), quantum disordered region (QDR), and quantum critical region (QCR) (Fig. 1).

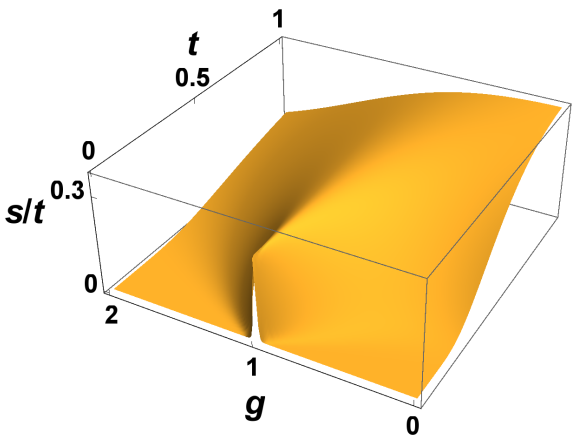

FIG. 2: The entropy (divided by t) as a function of the reduced temperature t and reduced transverse field g. When the temperature is high the entropy maxima deviate from the line $g_c = 1$, but when the temperature is low the maxima of entropy appear near the QCP.

A. Classical and Quantum disordered regions

The CDR and QDR in the 1DTFIM are qualitatively characterized by $|g-1|/t \gg 1$. In these two regions the free energy density takes the form

$$f_I \approx E(g) - \frac{t}{\pi}\int_0^\pi e^{-2A} dk \tag{13}$$

with $A = \sqrt{1 + g^2 - 2g\cos k}/t$, and $E(g) = -\frac{1}{\pi}\int_0^\pi \sqrt{1 + g^2 - 2g\cos k} dk$ as its ground state energy density in unit of J. The temperature-dependent information is encoded in the integral of Eq. (13) which can be asymptotically performed via the steepest descent method[38,39],

$$\frac{t}{\pi}\int_0^\pi e^{-2A} dk \approx \frac{t^2}{\sqrt{2\pi g}} f\left(\frac{|1-g|}{t}\right) \tag{14}$$

with the universal scaling function $f(|1-g|/t) = (|1-g|/t)^{1/2} e^{-2|1-g|/t}$. Therefore in the CDR and QDR, the leading contribution to the free energy density becomes

$$f_I - E(g) \approx -\frac{|1-g|^2}{\sqrt{2\pi g}}\left(\frac{t}{|1-g|}\right)^{3/2} e^{-\frac{2|1-g|}{t}}. \tag{15}$$

Although Eq. (15) includes an exponentially thermal suppression term, it still is consistent with the general hyperscaling ansatz for the free energy in Eq. (2). From Eq. (15), we can readily determine the critical scaling behaviors of various thermodynamic quantities to the lead-

ing term as follows

$$s \approx \sqrt{\frac{2}{\pi g}} |g-1|^{3/2} t^{-1/2} e^{-\frac{2}{t}|1-g|}; \quad (16)$$

$$c_v \approx \sqrt{\frac{2\pi t}{g/|1-g|}} \left(\frac{|g-1|}{t}\right)^2 e^{-\frac{2}{t}|1-g|}; \quad (17)$$

$$\alpha \approx \sqrt{\frac{2\pi t}{g/|1-g|}} \frac{|g-1|}{t^2} e^{-\frac{2}{t}|1-g|} \mathrm{sgn}(g-1); \quad (18)$$

$$\Gamma_{cr}(t \to 0, g) \approx \frac{\alpha}{c_v} = \frac{\mathrm{sgn}(g-1)}{|g-1|}. \quad (19)$$

The Grüneisen ratio in Eq. (19) is clearly divergent when approaching the QCP in the CDR or QDR at low temperatures. A direct result of Eq. (19) is that at low temperatures the entropy is maximized near the QCP when the control parameter g is tuned to across the QCP, at $g_c = 1$, as discussed in Sec. II. Fig. 2 explicitly shows the maximization of the entropy near the QCP.

B. Quantum critical region

When the system stays in the QCR, one immediately obtains $\Gamma_{cr}(t, g = 1) = 1/2$, which deviates from the scaling prediction of Eq. (4). In order to understand this result, we note that the scaling prediction of Eq. (4) has been made based on the assumption[13] that the linear term in the scaling expansion series of Eq. (3) in powers of $r/(T/T_0)^{1/(\nu z)}$ is nonzero. When the linear scaling term vanishes, we need to expand the series to the sub-leading terms, and this may yield different critical behaviors beyond the prediction of Eq. (3). Indeed, from the the scaling form of the free energy in the QCR of the 1DTFIM, the linear scaling term vanishes and the quadratic one appears as the leading contribution, resulting in a classical-like constant scaling behavior for the Grüneisen ratio Γ_{cr} near the QCP in the QCR (the vanishing of G_T in Eq. (4) for 1DTFIM is also obtained in Ref. [36] following a different analysis).

In the QCR, $|1-g| \ll t$ is a natural constraint. We work in the low-temperature limit. We note that $A = ((1-g)^2/t^2 + 4g\sin^2(k/2)/t^2)^{1/2}$, and, moreover, there is a crossover $k_c \approx t$ such that when $k < k_c$, $|\sin(k/2)|/t \ll 1$ and when $k > k_c$, $|\sin(k/2)|/t \gg 1$. Correspondingly, we split the integration in the expression for the free energy into two parts,

$$f_I = -\frac{t}{\pi}\left(\int_0^{k_c} + \int_{k_c}^{\pi}\right) dk \ln\left(e^A + e^{-A}\right). \quad (20)$$

We only consider the low-lying contributions from $k < k_c$, then $\sqrt{\left(\frac{1-g}{t}\right)^2 + 4g\left(\frac{\sin(k/2)}{t}\right)^2} \ll 1$. As a result,

$$-\frac{t}{\pi}\int_0^{k_c} dk \ln\left(e^A + e^{-A}\right) \overset{k_c \approx t}{\approx} -\frac{t^2}{\pi}\left(a_g + \frac{1}{2}\left(\frac{1-g}{t}\right)^2\right), \quad (21)$$

where $a_g = (g/6 + \ln 2)$. It follows that in the low-temperature limit in the QCR,

$$f_I \sim -t^2\left(a_g + \frac{1}{2}\frac{(1-g)^2}{t^2}\right), \quad (22)$$

which is consistent with the hyperscaling ansatz. However, the leading scaling term is quadratic in the expansion parameter $(1-g)/t$. From Eq. (22) we obtain

$$s \sim (2\ln 2 + \frac{g}{3})t \Rightarrow \begin{cases} \alpha \sim t/3 \\ c_v \sim (g/3 + 2\ln 2)t \end{cases} \quad (23)$$

and (g is fixed near critical point)

$$\Gamma_{cr} = \frac{\alpha}{c_v} \sim \text{constant}. \quad (24)$$

We have thus provided the understanding for the Güneisen ratio reaching a constant in the QCR, $|1-g| \ll t$. The case we considered earlier, $g = g_c = 1$, falls in this regime. The contradiction with the usual scaling prediction of Eq. (4) is only apparent. Generically, in each regime (such as QCR, CDR or QDR), we can express the scaling function of the free energy in terms of a scaling variable that is small in that regime [*c.f.* Eq. (2) for the CDR and QDR, and Eq. (3) for the QCR], and we expect that the leading linear term in the Taylor expansion is nonzero. Eqs. (4,5) then follows. However, it is special for the 1DTFIM in all regions. For the CDR or QDR, corresponding to $t/|g-g_c| \ll 1$, the leading term actually exponentially decays (Eq. (14)). Nevertheless the obtained Grüneisen ratio still respects the general analysis Eq. (5), though the combined exponents for the coefficient G_r in Eq. (5) can not apply to the 1DTFIM. By contrast, the scaling function in the QCR indeed has a Taylor expansion form. However, we have shown that, for the QCR of the 1DTFIM, the linear term in the Taylor expansion of the scaling function for the free energy, $f(|1-g|/t)$ vanishes. The leading non-vanishing term is quadratic, which leads to the apparent violation of Eq. (4) in the QCR. (We believe that this mechanism also applies to the anisotropic XY model, in which a similar constant behavior of the Grüneisen ratio arises in the QCR[40].) We stress that our analysis for the 1DTFIM makes it clear that the the hyperscaling form for the singular part of the free energy introduced in Ref. [13] still applies here. The constant behavior of the Grüneisen ratio in the QCR does not violate the scaling form of the free energy, but is a reflection of a unique form of the scaling function.

V. CROSSOVER SCALING OF THERMODYNAMIC QUANTITIES

Based on different dominant factors, the phase diagram of the 1DTFIM can be qualitatively divided into three regions: the low-temperature CDR, QDR, and the

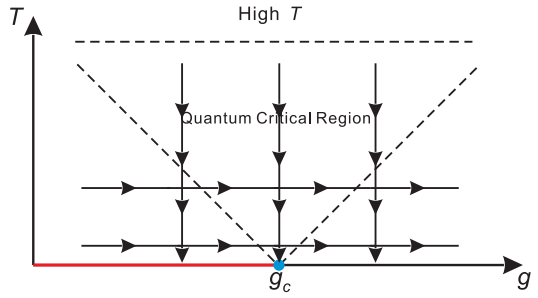

FIG. 3: The horizontal (vertical) lines of arrows denote tuning control parameters (temperatures) across different regions of the 1DTFIM at fixed temperatures (tuning parameters).

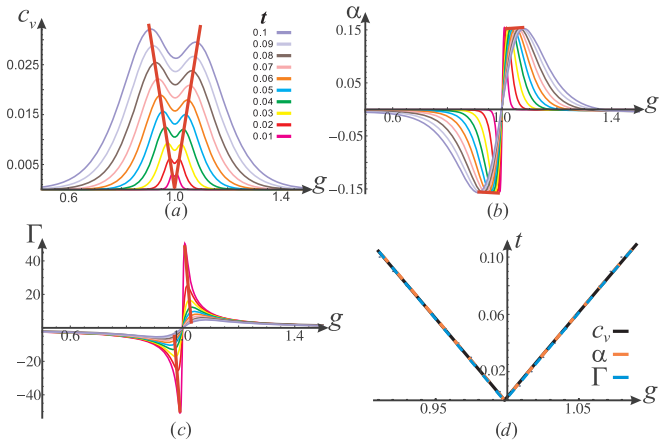

FIG. 4: The crossover scaling behaviors of the specific heat [Fig. 4(a)],magnetic expansion coefficient [Fig. 4(b)], the Grüneisen ratio [Fig. 4(c)]. The control parameter g varies in the range $(0.5, 1.5)$. The extrema in the figures for each thermodynamic quantity at each fixed t are illustrated by the red solid line. Those extrema are then plot on the $g-t$ plane to identify the corresponding line of the crossover, which are shown in Fig. 4(d). The crossover lines for c_v, α, and the Grüneisen ratio can be fitted as $t = 8\times10^{-5}+1.16|g-1.00|^{0.99}$, $t = 7\times10^{-5}+1.17|g-1.00|^{0.99}$, and $t = 8\times10^{-5}+1.18|g-1.00|^{0.99}$, respectively. The exponent 0.99 very close to the exact scaling exponent 1. The crossover lines almost overlap with each other.

QCR, as shown in Fig. 1. Near the boundaries of the different regions, there is a strong competition between the thermal and quantum fluctuations and, as a result, crossover signatures are expected in physical properties as we tune the transverse field or temperature across the boundaries. In the following we shall demonstrate that there indeed exist crossover scaling behaviors in the 1DTFIM for the specific heat and magnetic expansion coefficient. However, subtleties emerge for the Grüneisen ratio in the QCR.

A. Crossover at Fixed Temperatures

Consider first the isothermal behavior as illustrated in Fig. 3, where each horizontal line of arrows illustrates tuning the transverse magnetic field through the different regions of the phase diagram at a fixed (low) temperature t. The results are plotted in Figs. 4(a,b,c). They show that the thermodynamic quantities of the 1DTFIM reach extrema when g is tuned across the boundaries of the different regions. The crossover scaling exponent extracted from the numerical results of Figs. 4(d) is 0.99 which agrees well with the universal scaling exponent in the 1DTFIM, $z\nu = 1$. The minor deviation of the exponent from the exact value is because when the temperature is relatively high the thermal fluctuations become stronger such that those crossover signatures in the crossover are weakened, making it harder to precisely locate the crossover. However, the deviation is negligible, indicating the existence of a large region of quantum criticality in the 1DTFIM, which is consistent with the conclusions drawn from a recent NMR experiment on the quasi-1D ferromagnet $CoNb_2O_6$[19].

B. Crossovers at Fixed Control Parameters

The crossovers at fixed g are illustrated in Fig. 3, where each vertical line of arrows represents temperatures tuning across different regions at a fixed tuning parameter g. Similarly, we use the extrema in Figs. 5(a,b,c,d,e,f) to extract the crossover of c_v, α and the Grüneisen ratio. Fig. 5(g) shows that the crossover scaling of the specific heat coefficient and magnetic expansion coefficient are consistent with the scaling prediction with scaling exponent $\nu z = 1$. It is also coincident with previous discussions on the crossover scalings with tuning control parameters at fixed temperatures. However, for the Grüneisen ratio, its crossover scaling exponent significantly deviates from the general crossover scaling argument, as it is shown in Fig. 5(g). The crossover scaling with power-law fitting gives rise to an exponent of 1.18, which is about 20% larger than the exact value! This reflects the weaker form of the critical singularity in the Grüneisen ratio as a function of temperature, as we discussed in Sec. IV B and seen in Fig. 5(g).

VI. DISCUSSION AND CONCLUSIONS

In this paper, we have studied in some detail the scaling behavior of thermodynamic properties in the 1DTFIM at low temperatures. The results are unusual and can serve as telltale signs of the 1DTFIM: the Grüneisen ratio is power-law divergent following the conventional scaling analysis when the system is tuned across the QCP as a function of the non-thermal control parameter (the transverse magnetic field) at zero temperature; by

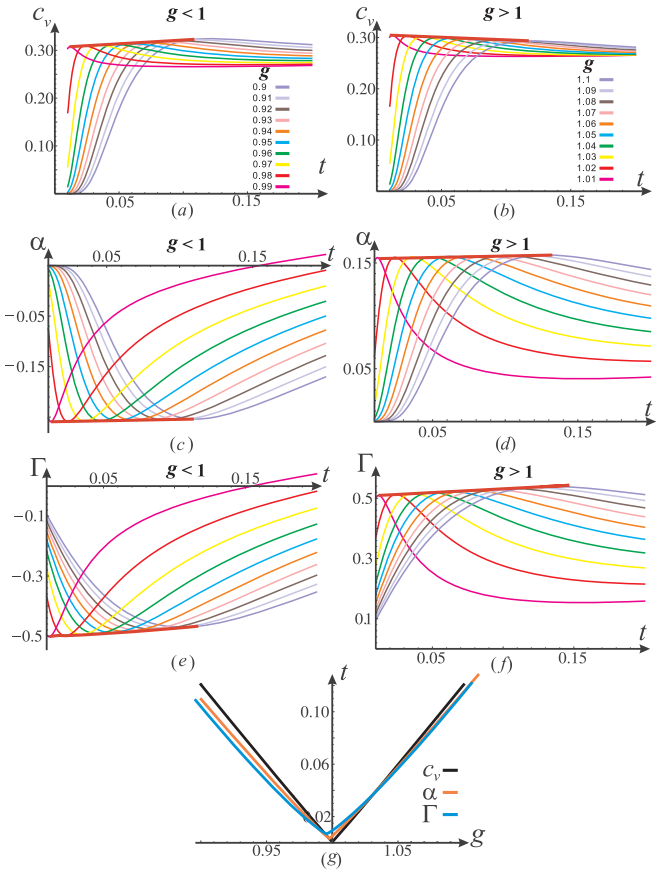

FIG. 5: The crossover scaling behaviors of the specific heat [Figs. 5(a,b)], magnetic expansion coefficient [Figs. 5(c,d)], and Grüneisen ratio [Figs. 5(e,f)]. The temperature is set in the range $(0.01, 0.2)$. The extrema in the figures for each thermodynamic quantity at each fixed g are illustrated by the red solid line. Those extrema are then plot on $g-t$ plane to fit the crossover scaling behaviors, shown in Fig. 5(g). The crossover scaling for c_v, α, and Γ fit as $t = 6\times10^{-4}+1.27|g-1.00|^{1.02}$, $t = 0.003+1.38|g-1.00|^{1.07}$, and $t = 0.007+1.73|g-0.99|^{1.18}$, respectively.

contrast, it approaches a constant when the QCP is approached with a decreasing temperature in the quantum critical region.

We clarified the reasons for this unusual feature. The singular part of the free energy satisfies the form introduced earlier (Ref. [13]). However, its scaling function is unique in that, in the quantum critical region (but not in the quantum disordered or classical disordered region), the scaling function can be Taylor expanded and its linear term vanishes. This unsual form of the scaling function makes the temperature dependence of the Grüneisen ratio in the quantum critical region to differ from the generic expectations of the scaling analysis. In the quantum disordered and classical disordered regions, the leading behavior of the scaling functions is dominated by a peculiar exponential form different from the usual Taylor expansion one. Despite of lacking simple combined exponents for G_r (Eq. (5)) used in Ref. [13], the obtained power-law divergent form of the Grüneisen ratio as a function of the non-thermal control parameter still respects the results obtained in these two regimes. Consequently, entropy is enhanced as the transverse field is tuned to its critical value at low but nonzero temperatures, as expected from generic scaling analysis.

We have also discussed the crossover behavior of the specific heat, magnetic expansion coefficient and the Grüneisen rato. The contrast between the critical behavior of the Grüneisen ratio between the quantum critical and quantum or classical disordered regions is also manifested in how the thermodynamic quantities capture the crossovers when they are approached from different directions in the phase diagram of temperature and transverse magnetic field.

The one-dimensional transverse-field Ising model is a paradigmatic theoretical model for quantum criticality, and our work clarifies the singularities, scaling and crossover of the thermodynamic quantities in this model. Given the wide interest in quantum criticality, it would be important to have actual materials that realize the one-dimensional transverse-field Ising model. At the present time, the materials which are well-established to be describable by the one-dimensional transverse-field Ising model is still rare. The unique forms of critical scaling and crossover we have determined in this work will serve as signatures to experimentally identify materials that realize this prototype model system for quantum criticality. Finally, the one-dimensional transverse-field Ising model can be transformed to free fermionic model [Eqs. (7, 8)], ergo, our results can also shed light on understanding the critical scaling behaviors in the relevant fermionic model.

Note added: After this work was completed, we learnt the experimental studies in a quasi-one-dimensional material had provided evidences to support our scaling predictions [41].

VII. ACKNOWLEDGMENT

We would like to acknowledge useful discussions with Zhe Wang and Robert-Jan Slager. This work was in part supported by the NSF grant No. DMR-1611392 and the Robert A. Welch Foundation Grant No. C-1411. Q.S. acknowledges the hospitality of the Aspen Center for Physics (the NSF Grant No. PHY-1607611). Two of us (L.Z. and Q.S.) would like to thank M. Garst and A. Rosch for an earlier collaboration (Ref. [13]) on this general topic.

[1] Special issue on Quantum Phase Transitions, J. Low Temp. Phys. **161**, 1 (2010).
[2] S. Sachdev, *Quantum PhaseTransitions* (Cambridge University Press, Cambridge, 2011), 2nd ed.
[3] P. Coleman and A. J. Schofield, Nature **433**, 226 (2005).
[4] Q. Si and F. Steglich, Science **329**, 1161 (2010).
[5] J. A. Hertz, Phys. Rev. B **14**, 1165 (1976).
[6] S. Chakravarty, B. I. Halperin, and D. R. Nelson, Phys. Rev. B **39**, 2344 (1989).
[7] A. J. Millis, Phys. Rev. B **48**, 7183 (1993).
[8] P. Merchant, B. Normand, K. Krämer, M. Boehm, D. McMorrow, and C. Rüegg, Nat. Phys. **10**, 373 (2014).
[9] E. Schuberth, M. Tippmann, L. Steinke, S. Lausberg, A. Steppke, M. Brando, C. Krellner, C. Geibel, R. Yu, Q. Si, et al., Science **351**, 485 (2016).
[10] J. Wu, Q. Si, and E. Abrahams, Phys. Rev. B **93**, 104515 (2016).
[11] J. Wu, F. Zhou, and C. Wu, Phys. Rev. B **96**, 085140 (2017).
[12] E. Grüneisen, Annalen der Physik **344**, 257 (1912).
[13] L. Zhu, M. Garst, A. Rosch, and Q. Si, Phys. Rev. Lett. **91**, 066404 (2003).
[14] L. D. Landau and E. M. Lifshitz, *Statistical physics* (Pergamon, 1968).
[15] P. Gegenwart, Q. Si, and F. Steglich, Nat. Phys. **4**, 186 (2008).
[16] J. Wu, L. Zhu, and Q. Si, J. Phys.: Conf. Ser. **273**, 012019 (2011).
[17] A. Rost, R. Perry, J.-F. Mercure, A. Mackenzie, and S. Grigera, Science **325**, 1360 (2009).
[18] K. Grube, S. Zaum, O. Stockert, Q. Si, and H. v. Löhneysen, Nat. Phys. **13**, 742 (2017).
[19] A. W. Kinross, M. Fu, T. J. Munsie, H. A. Dabkowska, G. M. Luke, S. Sachdev, and T. Imai, Phys. Rev. X **4**, 031008 (2014).
[20] T. Niemeijer, Physica **36**, 377 (1967).
[21] P. Pfeuty, Ann. Phys. **57**, 79 (1970).
[22] E. Barouch and B. M. McCoy, Phys. Rev. A **3**, 786 (1971).
[23] M. Suzuki, Prog. Theor. Phys. **46**, 1337 (1971).
[24] M. Suzuki, Prog. of Theor. Phys. **56**, 1454 (1976).
[25] R. Jullien, P. Pfeuty, J. Fields, and S. Doniach, Phys. Rev. B **18**, 3568 (1978).
[26] A. Kopp and S. Chakravarty, Nat. Phys. **1**, 53 (2005).
[27] R. Coldea, D. Tennant, E. Wheeler, E. Wawrzynska, D. Prabhakaran, M. Telling, K. Habicht, P. Smeibidl, and K. Kiefer, Science **327**, 177 (2010).
[28] J. Wu, M. Kormos, and Q. Si, Phys. Rev. Lett. **113**, 247201 (2014).
[29] J. H. H. Perk, H. Capel, G. Quispel, and F. Nijhoff, Physica A: Statistical Mechanics and its Applications **123**, 1 (1984).
[30] A. B. Zamolodchikov, Int. J. Mod. Phys. A **4**, 4235 (1989).
[31] V. A. Fateev, Phys. Lett. B **324**, 45 (1994).
[32] G. Delfino, G. Mussardo, and P. Simonetti, Nucl. Phys. B **473**, 469 (1996).
[33] P. Fonseca and A. Zamolodchikov, J. Stat. Phys. **110**, 527 (2003).
[34] S. T. Carr and A. M. Tsvelik, Phys. Rev. Lett. **90**, 177206 (2003).
[35] J. H. H. Perk and H. Au-Yang, J. Stat. Phys. **135**, 599 (2009).
[36] M. Garst and A. Rosch, Phys. Rev. B **72**, 205129 (2005).
[37] S. Katsura, Phys. Rev. **127**, 1508 (1962).
[38] Z. Wang and D. Guo, *An introduction to special functions* (Peking University Press, Beijing, 2000).
[39] M. A. Lavrentieff and B. V. Shabat, *Methods of functions of a complex variable* (Higher Educational Press, Beijing, 2006).
[40] M. Zhitomirsky and A. Honecker, J. Stat. Mech.: Theor. and Exp. **2004**, P07012 (2004).
[41] Z. Wang, T. Lorenz, D. Gorbunov, P. Cong, Y. Kohama, S. Niesen, O. Breunig, J. Engelmayer, A. Herman, J. Wu, et al., Phys. Rev. Lett. **120**, 207205 (2018).